

EFFECTS OF NEODYMIUM DOPING ON DIELECTRIC AND OPTICAL PROPERTIES OF $\text{Ba}_{(1-x)}\text{Nd}_x\text{Ti}_{1.005}\text{O}_3$ CERAMICS

WENXING ZHANG*, **, #LIXIN CAO*, WENWEN WANG*, GE SU*, WEI LIU*

*College of Material Science and Engineering, Ocean University of China, Qingdao, 266100, P.R.China

**Shangqiu Normal University, Shangqiu, HeNan Province, 476000, P.R.China

#E-mail: caolixin@ouc.edu.cn

Submitted September 18, 2012; accepted June 16, 2013

Keywords: Barium titanate ceramics, Nd^{3+} content, Dielectric and optical properties

This paper investigated the optical properties and dielectric properties of neodymium doped BaTiO_3 ceramics prepared by $\text{Ba}_{(1-x)}\text{Nd}_x\text{Ti}_{1.005}\text{O}_3$ powders synthesized via a hydrothermal method. The effects of Nd^{3+} ions content on the structure, dielectric properties and optical properties of the ceramics were studied. The structural analysis performed on the X-ray diffractometer shows that the phase compositions of all ceramics are tetragonal phase structure. The red shift of the absorption edge indicates the presence of defect energy levels which was proved by the UV-Vis-NIR diffuse reflection spectra. Dielectric property measurements show that Nd-doped BaTiO_3 ceramics possess improved dielectric properties at low Nd^{3+} contents ($x = 0.001$ and 0.002), as demonstrated by decreased dependence to frequency for both the dielectric constant and dielectric loss.

INTRODUCTION

The ferroelectric BaTiO_3 is a widely studied electroceramic that can be deployed in various areas such as optical, electric, thermistors, tunable microwave devices and multilayer ceramic capacitors due to its excellent characteristics [1-5]. By adding different dopants to BaTiO_3 , many characteristics for various applications can be obtained. The dielectric properties of BaTiO_3 ceramic can be modified by doping with different metal cations. By means of doping with Sr and La, high dielectric constant ceramics at room temperature have been achieved [6]. Doping of Mg led to the decrease of Curie temperature and the dielectric constant at peak temperature [7]. Among the metal cations, neodymium is an interesting dopant. It has been observed that Nd^{3+} can replace Ba^{2+} and Ti^{4+} in BaTiO_3 [8-10]. It was reported that Ba-rich samples will drive amphoteric dopants to more frequently occupy B-sites, and Ti-rich samples will drive such dopants more frequently into the A-sites [11]. The dielectric constant of Nd-doped BaTiO_3 ceramics which were pressed into disks with 10mm in diameter and about 1mm in thickness synthesized by conventional powder processing method increases significantly by adding Nd^{3+} with Ba/Ti molar ratio increasing [9]. With increasing Nd doping levels in BaTiO_3 ceramics prepared by sol gel method, the phase transition of tetragonal to cubic structure appears [10]. It proves that Nd is a phase change inhibitor. The Nd^{3+} doped barium zirconium titanate ceramics exhibit negative temperature coefficient of resistance (NTCR) and the diffuse phase transition behavior at higher Nd^{3+} content [12].

Considering the importance applications of BaTiO_3 ceramic in electronic devices and there is scarce systematic research on the effects of Nd doping content. The objective of the research was set to study the dielectric and optical properties. In this paper, we hope that neodymium occupies Ba sites and the Ti/Ba molar ratio of 1.005 was used for experiments. A series of $\text{Ba}_{(1-x)}\text{Nd}_x\text{Ti}_{1.005}\text{O}_3$ ceramics ($x = 0.0005, 0.001, 0.002, 0.005, 0.01, 0.02$ and 0.05) were prepared. The ceramic samples were fabricated from powders synthesized by hydrothermal method. The influences of Nd content on the structure, dielectric properties and optical properties were investigated.

EXPERIMENTAL

Pure and Nd-doped BaTiO_3 were synthesized in 23 ml Teflon lined autoclaves at 180°C for 12 hours by hydrothermal method. The required amount of barium chloride dehydrate ($\text{BaCl}_2 \cdot 2\text{H}_2\text{O}$ (A.R.)), tetrabutyl titanate ($\text{Ti}(\text{OC}_4\text{H}_9)_4$ (C.P.)) and neodymium chloride ($\text{NdCl}_3 \cdot 6\text{H}_2\text{O}$ (2.5N.)) corresponding to the composition of $\text{Ba}_{(1-x)}\text{Nd}_x\text{Ti}_{1.005}\text{O}_3$ were precisely measured. First, $0.01(1-x)$ ($x = 0, 0.0005, 0.001, 0.002, 0.005, 0.01, 0.02$ and 0.05) mol $\text{BaCl}_2 \cdot 2\text{H}_2\text{O}$ were added to 10 ml deionized water with continuously stirring at 80°C to prepare aqueous solution. 0.01005 mol $\text{Ti}(\text{OC}_4\text{H}_9)_4$ was added to the above solution drop by drop under quick stirring. Then 0.05 mol NaOH (A.R.) and $\text{NdCl}_3 \cdot 6\text{H}_2\text{O}$ weighed in stoichiometric proportions were added to above solution respectively. After stirring for 30 min, the

mixtures were transferred into Teflon-lined autoclaves filled with deionized water of 80°C until a filling degree of 80 % was reached. The hydrothermal reaction was carried out in an oven. After the reaction, the autoclaves were cooled to room temperature, pure and Nd-doped $BaTiO_3$ powders were washed with deionized water several times to remove the absorbed impurities and the products were oven dried at 90°C for 12 h. For $BaTiO_3$ ceramic studies, the as-prepared $BaTiO_3$ powders were sintered at 1150°C in air for 2 h. For dielectric studies, 400 mg of the resulting powders was ground with 2 ml aqueous solution of polyvinyl alcohol (1 mg/ml), and then the slurries were allowed to dry at 90°C for 10 h under atmosphere. The dried powders were then reground and pressed with an applied load of 6.5 MPa into disks of 13 mm in diameter and 2 mm in height. The samples were sintered at 1150°C in air for 2 h. Colloidal silver paint (SPI, Inc.) was applied to both faces before annealing the pellets at 100°C for 1 h.

X-ray powder diffraction measurements were performed on the X-ray diffractometer (XRD, Model DX2700) using a $Cu K\alpha$ ($\lambda = 1.54 \text{ \AA}$) radiation source. Cell parameters of the samples were refined by the least squares' fitting method based software unitcell-97. The morphology was analyzed using scanning electron microscopy (SEM, VEGA3 TESCAN). The measurements of FT-IR spectrum were carried out by means of Nicolet Avator 360. The diffuse reflection spectra in the UV, Visible, and near IR regions were recorded with a Hitachi U4100 spectrophotometer. Dielectric properties were measured on an Agilent 4294A impedance analyzer with a frequency sweep of 40 Hz - 5 MHz.

RESULTS AND DISCUSSION

The XRD patterns of pure and Nd-doped $BaTiO_3$ ceramics are shown in Figure 1. It is obvious that pure $BaTiO_3$ ceramics fit well with the tetragonal phase of $BaTiO_3$ $P4mm$ space group (JCPDF No.05-0626). The characteristic peaks of tetragonal (200) and (002) are observed at about 45° and grow gradually weaker with the increase of Nd^{3+} content. The result indicates that higher x values will restrain the phase change from cubic to tetragonal. When $x = 0.05$, a main phase with

tetragonal phase and traces of a secondary phase of $BaCO_3$ and $BaTi_2O_5$ (JCPDF No.34-0133) are observed and the stations have been indexed. It was reported that different phases such as $BaTiO_3$, $BaCO_3$ and $BaTi_2O_5$ can coexist in $BaTiO_3$ ceramics. The $BaCO_3$ formation can be introduced through the contamination of CO_2 from the atmosphere, the impure phase $BaCO_3$ decreases with increasing the sintering temperature [13-15]. It is believed that the metastable $BaTi_2O_5$ phase formed in Ti-rich condition at high temperature [14]. It was reported that the position of the (002) and (200) peaks are slightly shifted towards the larger Bragg angle when Nd content increases [10], the result is accordant with the report in this experiment. In Figure 1, the diffraction peak intensity becomes weak in comparison with others when $x = 0.05$ and it maybe caused by other phases in $BaTiO_3$. The lattice parameter and unit cell volume of the $BaTiO_3$ ceramics were calculated from the XRD data and are given in Table 1. The data shows that the c parameters and unit cell parameters decrease, indicating that Nd^{3+} is incorporated into the crystal lattice of $BaTiO_3$. The unit cell volume decreases with the increase of Nd^{3+} content. This is attributed to the fact that the ionic radius of Nd^{3+} is smaller than that of Ba^{2+} [16, 17]. The tetragonality, defined as the ratio c/a of the lattice parameters [18], decreases with the increase of Nd^{3+} content.

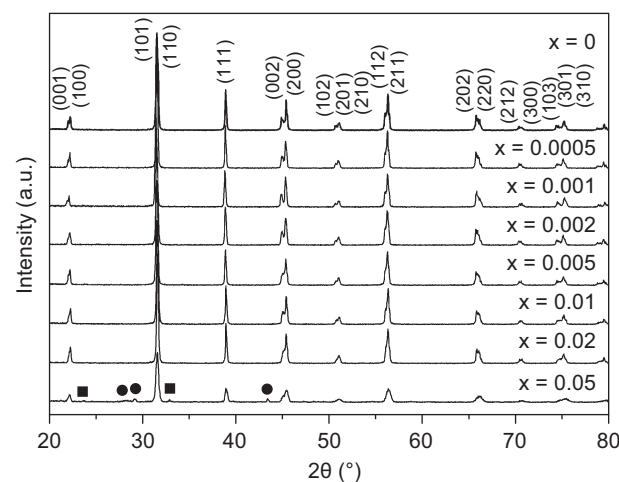


Figure 1. XRD pattern of $Ba_{(1-x)}Nd_xTi_{1.005}O_3$ ceramics ($x = 0, 0.0005, 0.001, 0.002, 0.005, 0.01, 0.02$ and 0.05).

Table 1. Crystal system, lattice parameter, unit cell volume.

System	Composition, x	crystal system	$a(\text{\AA})$	$c(\text{\AA})$	c/a	cell volume (\AA^3)
$Ba_{(1-x)}Nd_xTi_{1.005}O_3$	0	Tetragonal	3.984	4.027	1.011	63.918
	0.0005	Tetragonal	3.999	4.031	1.008	64.464
	0.001	Tetragonal	3.999	4.030	1.008	64.448
	0.002	Tetragonal	3.998	4.03	1.008	64.416
	0.005	Tetragonal	3.997	4.03	1.008	64.383
	0.01	Tetragonal	3.996	4.029	1.008	64.335
	0.02	Tetragonal	3.997	4.026	1.007	64.319
	0.05	Tetragonal	3.99	4.004	1.004	63.744

Figure 2 shows the SEM micrographs of pure and Nd-doped BaTiO₃ ceramics sintered at 1150°C in air for 2 h. As can be seen from Figure 2, the microstructure of pure BaTiO₃ exhibits large grain size, however the grain size of Nd-doped BaTiO₃ significantly decreases. The result suggests that the incorporation of Nd³⁺ can limit grain growth in the BaTiO₃ ceramics. This observed behavior is believed to be caused by the replacement mechanism of Ba²⁺ + 2Nd³⁺ = 2Ti⁴⁺ [19]. But when x value is 0.05, the grain size increases. We do not exactly know the reasons of such change on the morphology. One can suppose that the impurity expands grain boundaries,

which would cause increase of the grain size. In Figure 2, the porosity of Nd-doped BaTiO₃ is higher than pure BaTiO₃ ceramic. Therefore densities of Nd-doped ceramics are lower than that of pure BaTiO₃.

The FTIR spectra of BaTiO₃ ceramics doped with different Nd³⁺ content are shown in Figure 3. The absorption peak at about 524 cm⁻¹ is the characteristic of the Ti-O stretching vibrations in BaTiO₃ [20-22]. The peak at about 2.320 cm⁻¹ is due to ambient CO₂ [11]. In Figure 3, the bands of Nd-doped BaTiO₃ are sharper and stronger than that of pure BaTiO₃ and shift to higher wavenumbers. Figure 4 shows the UV-Vis-NIR diffuse

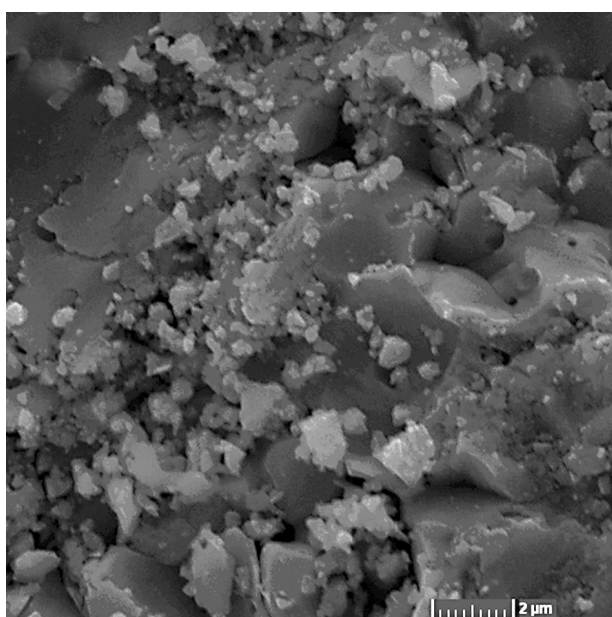
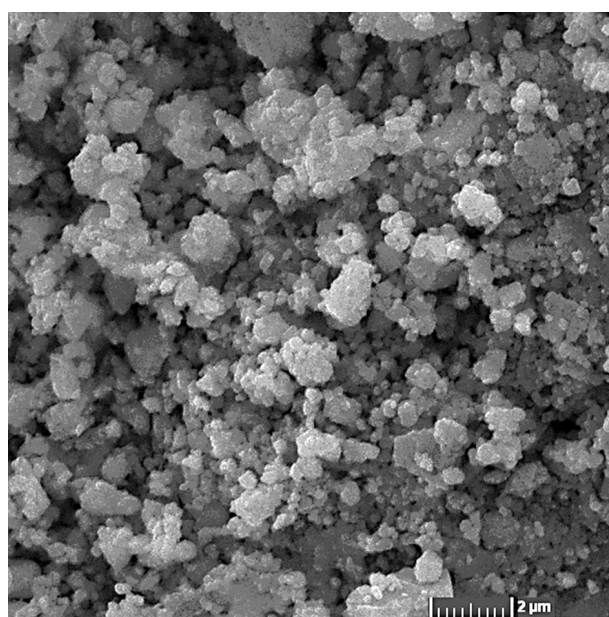
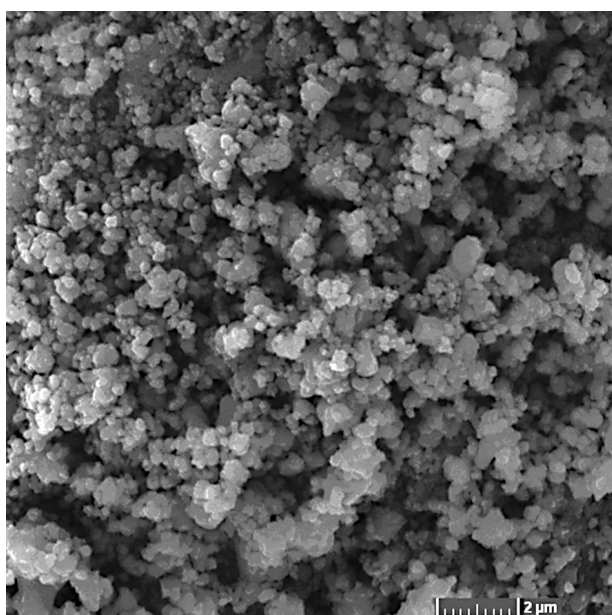
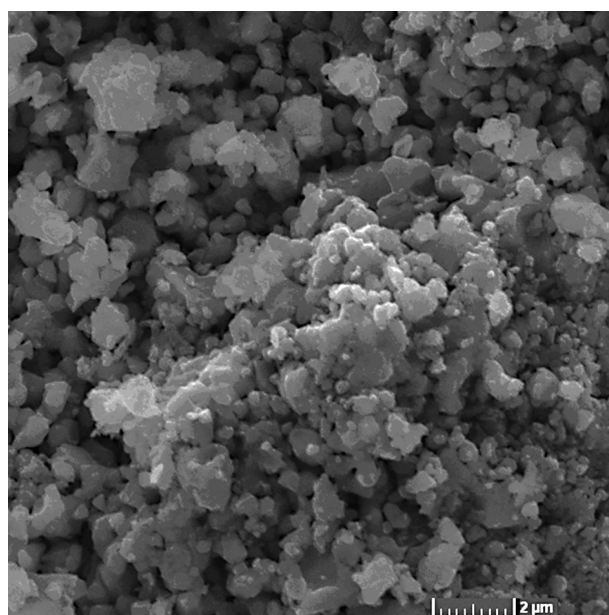
a) $x = 0$ b) $x = 0.0005$ c) $x = 0.005$ d) $x = 0.05$

Figure 2. SEM micrographs of Ba_(1-x)Nd_xTi_{1.005}O₃ ceramics sintered at 1150°C in air for different Nd³⁺ content. a) $x = 0$, b) $x = 0.0005$, c) $x = 0.005$ and d) $x = 0.05$.

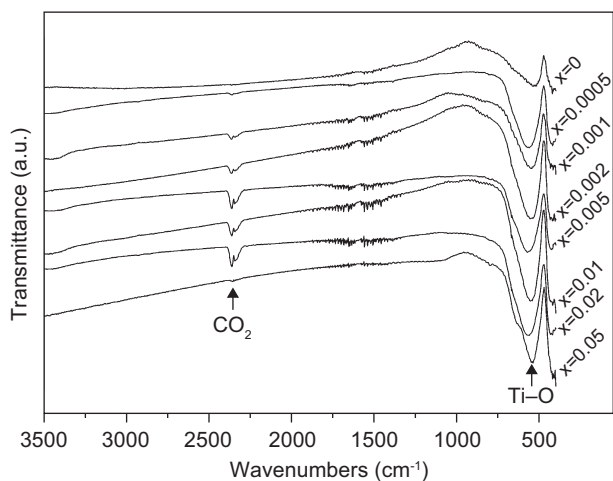


Figure 3. FTIR spectra of $Ba_{(1-x)}Nd_xTi_{1.005}O_3$ ceramics with different Nd^{3+} content.

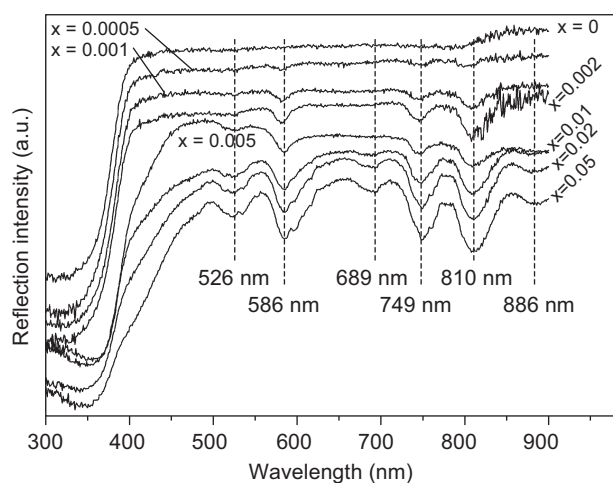
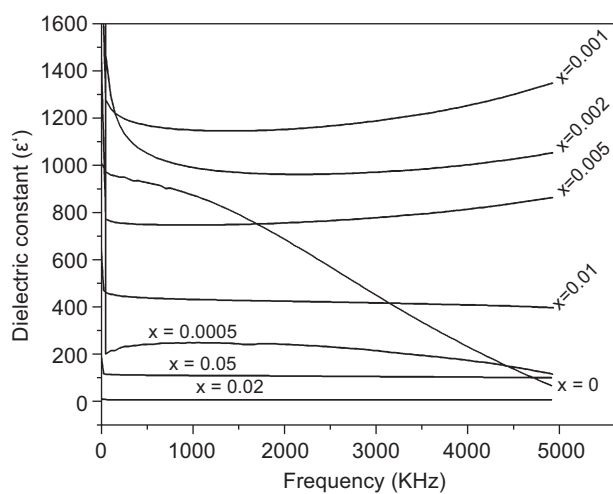
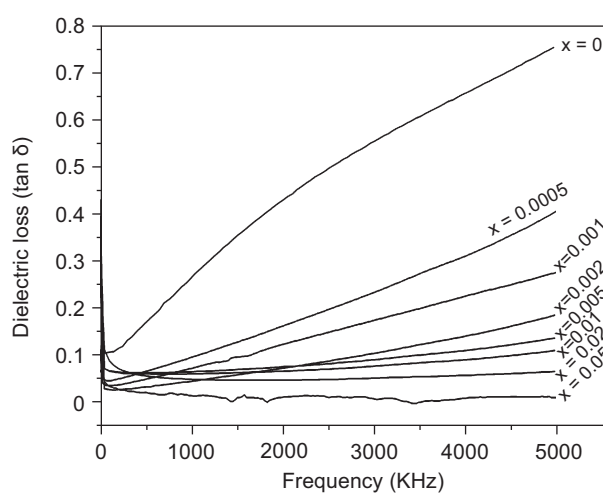


Figure 4. UV-Vis-NIR diffuse reflection spectra of $Ba_{(1-x)}Nd_xTi_{1.005}O_3$ ceramics.



a)



b)

Figure 5. Dielectric constant of $Ba_{(1-x)}Nd_xTi_{1.005}O_3$ ceramics as a function of frequency (a) and dielectric loss of $Ba_{(1-x)}Nd_xTi_{1.005}O_3$ as a function of frequency (b).

reflection spectra of $BaTiO_3$ ceramics with different Nd^{3+} content in the wavelength range of 300 - 900 nm. It can be seen that six characteristic absorption peaks of Nd^{3+} at 526 nm, 586 nm, 689 nm, 749 nm, 810 nm and 886 nm are observed and assigned to the electronic transitions of $^4I_{9/2} \rightarrow ^2G_{7/2}$, $^4G_{5/2}$, $^4F_{9/2}$, $^4S_{3/2}(^4F_{7/2})$, $^4F_{5/2}$, and $^4F_{3/2}$. It can be seen that the base-line reflections decrease with increasing Nd content and it can be caused by coarse surface of ceramic samples. The characteristic peaks become sharper and stronger with the x value increasing. But when x value is 0, no absorption peak can be observed. As shown in Figure 4, for Nd-doped $BaTiO_3$, their optical absorption edges shift to higher wavelength comparing to pure $BaTiO_3$ in the range of 300 - 370 nm. The red shift of the absorption edge indicates the presence of defect energy levels [3].

Figure 5a shows the influence of varying Nd^{3+} content in $BaTiO_3$ ceramic samples on dielectric constant over the frequency range of 40 Hz to 5 MHz. As can be seen in Figure 5a, the dielectric constant decreases evidently comparing with pure $BaTiO_3$ when x value is 0.0005. The decrease of Nd-doped $BaTiO_3$ grain size could be a possible reason for the dielectric constant decrease. When x value is 0.001, the dielectric constant increases dramatically and reaches a maximum value 1.312 at frequency of 5 MHz. It can be assumed that low content of Nd^{3+} is completely incorporated in the $BaTiO_3$ lattice. Further addition of Nd^{3+} above 0.001 leads to a rapid decrease in the dielectric constant. The change is possibly connected with the high porosity [23] and tetragonality decreasing with the increase Nd^{3+} contents as mentioned XRD results previously. But the dielectric constant is slightly increased when x value is 0.05, it can be associated with the increase of grain size as mentioned SEM result. Otherwise, the $Ba_{(1-x)}Nd_xTi_{1.005}O_3$ ceramics have far superior frequency stability with x value increasing and the result is similar to our previous report

[24]. The values of dielectric loss ($\tan \delta$) for various Nd^{3+} contents are shown in Figure 5b. When $x = 0$, the dielectric loss value of pure BaTiO_3 reaches maximum value 0.75 at frequency of 5 MHz. While the dielectric loss values are 0.41, 0.27, 0.18, 0.14, 0.11, 0.06 and 0.01 with x changing from 0.0005 to 0.05. It is obvious that Nd^{3+} content can dramatically affect the dielectric loss and the frequency stability increases over the range of 40 Hz - 5 MHz.

CONCLUSIONS

In summary, $\text{Ba}_{(1-x)}\text{Nd}_x\text{Ti}_{1.005}\text{O}_3$ ceramics with x value ranging from 0.0005 to 0.05 were investigated. All the BaTiO_3 ceramics show tetragonal structure. When x value is 0.05, the impurity phase of BaCO_3 and BaTi_2O_5 appears and confirmed by FTIR and XRD patterns. The UV-Vis-NIR diffuse reflection spectra prove that Nd^{3+} has been doped into BaTiO_3 . The dielectric constant decreases when $x = 0.0005$ comparing with pure BaTiO_3 ceramic. The maximum value of dielectric constant appears when x value is 0.001 and decreases with the increase of Nd^{3+} content. The dielectric properties of Nd-doped BaTiO_3 show frequency stability comparing with pure BaTiO_3 .

Acknowledgements

This work was supported by the Fundamental Research Funds for the Central Universities.

REFERENCES

1. Staedler D., Magouroux T., Rachid, Hadji, Joulaud C., Extermann J., Schwung S.: ACS. Nano 6, 2542 (2012).
2. Krowne C.M., Kirchoefer S.W., Chang W., Pond J.M., Alldredge L.M.B.: Nano. Lett. 11, 988 (2011).
3. Qin S.B., Liu D., Zuo Z.Y., Sang Y.H., Zhang X.L., Zheng F.F., Liu H., Xu X.G.: J. Phys. Chem. Lett. 1, 238 (2010).
4. Fang C.Y., Randal C.A., Lanagan M.T., Agrawal D.K.: J. Electroceram. 22, 125 (2009).
5. Swaminathan V., Pramana S.S., White T.J., Chen L., Chukka R.: Appl. Mater. Interf. 2, 3037 (2010).
6. Xu J., Liu H.X., He B., Hao H., Cao M.H.: Phys. Status. Solid. B 249, 1452 (2012).
7. Ren P.R., Fan H.Q., Wang X., Liu K.: Int. J. Appl. Ceram. Technol. 9, 358 (2012).
8. Hirose N., Skakle J.M.S., West A.R.: J. Electroceram. 3, 233 (1999).
9. Li Y.X., Yao X., Zhang L.Y.: Cream. Int. 30, 1325 (2004).
10. Rejab N.A., Sreekantan S., Razak K.A., Ahmad Z.A.: J. Mater Sci: Mater. Electron. 22, 167 (2011).
11. Dunbar T.D., Warren W.L., Tuttle B.A., Randall C.A., Tsur Y.: J. Phys. Chem. B 108, 908 (2004).
12. Sagar R., Madolappa S., Raibagkar R.L.: Solid State Sci. 14, 211 (2012).
13. Ghosh S., Dasgupta S., Sen A., Maiti H.S.: Mater. Lett. 61, 538 (2007).
14. Lee S., Randal C.A. Liu Z.K.: J. Am. Ceram. Soc. 92, 22 (2009).
15. Stojanovic B.D., Simoes A.Z., Paiva-Santos C.O., Jovalekic C., Mitic V.V., Varela J.A.: J. Eur. Ceram. Soc. 25, 1985 (2005).
16. Shannon R.D., Prewitt C.T.: Acta Crystall. B 1046 (1970).
17. Rai A.K., Rao K.N., Kumar L.V., Mandal K.D.: J. Alloy. Comp. 475, 316 (2009).
18. Buscaglia M.T., Harnagea C., Dapiaggi M., Buscaglia V., Pignolet A., Nanni P.: Chem. Mater. 21, 5058 (2009).
19. Cruickshank K.M., Jing X.P., Wood G., Lachowski E.E., West A.R.: J. Am. Ceram. Soc. 79, 1605 (1996).
20. Jin X.Q., Sun, D.Z. Zhang M.J., Zhu Y.D., Qian J.J.: J. Electroceram. 22, 285 (2009).
21. Reverón H., Aymonier C., Loppinet-Serani A., Elissalde C., Maglione M., Cansell F.: Nanotechnology 16, 1137 (2005).
22. Lazarević Z.Ž., Vijatović M., Dohčević-Mitrović Z., Romčević N.Ž., Romčević M.J., Paunović N., Stojanović B.D.: J. Eur. Ceram. Soc. 30, 623 (2010).
23. Hou R.Z., Ferreira P., Vilarinho P.M.: Chem. Matter. 2, 3536 (2009).
24. Zhang W.X., Cao L.X., Su G., Liu W.: J. Mater. Sci.: Mater. Electron. 24, 1801 (2013).